Molecular dynamics simulation of synchronization in driven particles

Tiare Guerrero* and Danielle McDermott†
Department of Physics, Pacific University, Forest Grove, OR 97116
(Dated: February 20, 2021)

Synchronization plays a key role in many physical processes. A particle may execute motion coordinated with position, a synchronization behavior that can be used to isolate complex natural behaviors, either with simulations or table-top experiments. We discuss a molecular dynamics simulation of a single particle moving through a viscous liquid driven across a washboard potential energy landscape. Our results show many dynamical patterns as we alter the landscape and driving force. Under certain conditions, the particle velocity and location are synchronized or phase-locked, forming closed orbits in phase space. Quasi-periodic motion is common, where the dynamical center of motion shifts the phase space orbit. We include molecular dynamics code to simulate and characterize particle dynamics.

I. INTRODUCTION

Synchronization is a universal phenomena in which individual oscillators change frequency due to external stimuli [1]. The flickering patterns of candle flames mediated by temperature fluctuations [3], vibrations of singing wineglasses interacting through sound waves [4], and metronomes vibrating through a supporting platform [5] are examples of in-phase coupled oscillations. Biological systems benefit from cooperative synchronization – birds coordinate wing flaps to optimize energy use during flight [6], frogs alternate croaking patterns [7], humans clap in time with music [8] and at a cellular level, neurons simultaneously fire in cardiac muscle [9] and brain tissue [10]. External forcing can cause or regulate synchronization – an electrical pacemaker regulates a heart beat and a pulsed light modifies the flashing pattern of fireflies .

Synchronized phase-locking or mode-locking first appeared in the scientific literature with Huygens' 1665 experiments on motions of synchronized pendula in wall-mounted clocks [2]. A locked-mode is an integer frequency ratio. In Huygens clocks, the pendula were observed swing at same rate – a 1:1 mode. For a higher modes, consider simple pendula of different lengths, a 2:1 mode occurs when a pendulum four times the length of another swings with twice the period.

Complex dynamics such as synchronized mode-locking can be studied with colloid particles in experiments or simulations. Typical colloids are plastic spheres suspended in de-ionized water or silica beads suspended in organic solvent. Because colloids are large and move slowly, particle position can be measured in real time with an optical camera [15]. Experimental measurements of step-by-step dynamics of colloids performing phase-locked motions are useful for understanding synchronization at a single particle level [27].

Light is a tool for manipulating the colloidal environment to alter synchronization patterns. Colloids can be trapped with radiation pressure from a laser beam [31]. A colloid centered in an optical trap is uniformly bombarded by photons. Off-center colloids experience a net force due to uneven photon collisions across the particle surface. Depending on the location of the particle in the trap, the radiation pressure either moves colloids toward center or ejects it from the trap. Diffraction gratings can create more complex light environments, such as periodic patterns of minima suitable for synchronization studies [30].

A single particle oscillator in a potential well is like a skateboarder in a half-pipe or a child on a swing. A confined oscillator may synchronize its location to the periodic pattern of the external drive, moving back and forth in time with the beat, or moving between substrate minima. A constant or dc drive the landscape modulates the particle velocity. Below some threshold the dc force is not strong enough to push the particle across a potential maximum so the average velocity is zero, a phenomena referred to as pinning [25]. Above the pinning threshold, a particle subject to a constant drive force will increase its speed at a rate propotional to the external drive. When the applied force varies periodically, the ac drive can cause the particle to hop back and forth across the landscape minima. Many synchronized patterns occur controlled by the substrate period, leading to mode-locking, where the average particle velocity is fixed for a range of dc drive forces [26].

Here we perform numerical studies on the synchronized dynamics of confined particles driven over a washboard shaped potential energy landscape. We describe our molecular dynamics model for a single particle in Section II. We choose this model for its relevance to condensed matter systems and ease of simulation. We summarize our results including synchronized motion of a single confined particle driven across a periodic landscape in Section III. We include exercises for interested students in Section IV. In Section V we describe how our results apply to physical systems such as dusty plasmas, superconducting vortices and Josephson junctions.

*Electronic address: guer9330@pacificu.edu
†Electronic address: mcdermott@pacific.edu

II. MOLECULAR DYNAMICS SIMULATION

We use a classical model for studying the dynamics of N interacting particles, using the net force on each particle to calculate its trajectory. Particles are confined in a two-dimensional (2D) simulation of area $A = L \times L$ where $L = 36.5a_0$ where a_0 is a dimensionless unit of length. An individual particle i has position $\vec{r}_i = x_i\hat{x} + y_i\hat{y}$ and velocity $\vec{v}_i = d\vec{r}_i/dt$. The edges of the system are treated with periodic boundary conditions such that a particle leaving the edge of the system is mapped back to a position within the simulation boundaries by the transformation $x_i + L \rightarrow x_i$ and $y_i + L \rightarrow y_i$. We show a schematic of the system in Fig. 1(a). The units of the simulated variables are summarized in Table I.

We confine the particles using a position dependent potential energy function, called a landscape or substrate. The landscape is modulated in the y-direction with the periodic function

$$U(y) = U_0 \cos(2\pi y/\lambda) \tag{1}$$

where $\lambda = L/N_p$ with N_p are the number of periods, and U_0 is an adjustable parameter to set the depth of the minima with simulation units of energy E_0. We plot this function in Fig. 1 for $N_p = 3$. In Fig. 1(a) we show the $x-y$ plane with a contour plot of $U(y)$ to illustrate the 2D potential energy landscape, where the maxima are colored red and the minima colored blue. The confining force on a particle i is calculated as $\vec{F}_i^l(\vec{r}_i) = -\nabla U_l(\vec{r}_i)$. In Fig. 1(b) we plot the function $U(y)$ to illustrate how the magnitude $\vec{F}_i^l$ is calculated from particle position y_i.

Particles are subject an external time-dependent driving force $\vec{F}^D(t)$ applied parallel to the y-direction. We model this force as

$$\vec{F}^D(t) = [F^{dc} + F^{ac}\sin(\omega t)]\hat{y}, \tag{2}$$

with a constant component F^{dc}, a time dependent component with amplitude F^{ac} and frequency $\omega = 2\pi f$.

The inertia of small particles is reduced by interactions with fluid particles [16]. In our model we assume colloids are overdamped – i.e. colloids are suspended in a continuous viscous fluid that dissipates energy such that the particles do not accelerate. Energy dissipation from the fluid is modeled with a frictional force on particle with velocity $\vec{v}_i$ as $\vec{F}_i^{drag} = -\eta\vec{v}_i$ with a friction coefficient η proportional to the fluid viscosity. We discuss friction models for spheres moving through fluids in Exercise IV A.

Newton's second law for an individual particle is simplified by the assumption $\vec{a}_i$ is zero. The overdamped equation of motion for an isolated particle is

$$\eta\vec{v}_i = \vec{F}_i^l(\vec{r}_i) + \vec{F}^D(t). \tag{3}$$

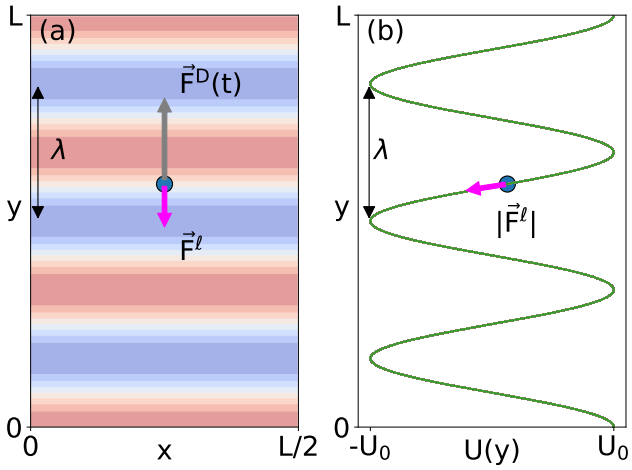

FIG. 1: Schematic of the simulation of a single particle driven across a washboard potential energy landscape. The period of the landscape is $\lambda = L/N_p$, where $N_p = 3$. The force due to the landscape is calculated from the gradient of the potential energy $\vec{F}^l = -\nabla U(\vec{r})$. (a) View of the $x-y$ plane. The time-dependent applied driving force $\vec{F}^D$ is parallel to the y-axis. The landscape is shown with a contour plot, with maxima in the potential energy marked in red and minima marked in blue. A particle is shown in the region between minima and maxima subject to competing forces of the landscape and applied driving force. (b) The potential energy function along the y-axis $U_l(y)$. The particle in (a) is shown at the same $y-$position. The slope of $U_l(y)$ is the magnitude of force $\vec{F}^l$.

with $\eta = 1$ in units of v_0/F_0. The equation of motion provides a direct calculation of the velocity of an individual particle from its location $\vec{r}_i$ and the simulation time.

The molecular dynamics simulation is controlled by a $for()$ loop which runs from an initial to maximum integer number of time steps. Each integer time step interval represents a simulation time of Δt simulation units τ. At each time step we evaluate the net force on each particle as a function of its position $\vec{r}_i(t)$ and then integrate the equation of motion to move particles to an updated position. Since the acceleration as zero, the integration of the equation of motion is performed via the Euler method

$$\vec{r}_i(t + \Delta t) = \vec{v}_i(t)\Delta t + \vec{r}_i(t) \tag{4}$$

for a small time step $\Delta t = 0.01\tau$. In Exercise IV C we describe the numerical methods for solving differential equations.

III. MODE-LOCKING OF A SINGLE PARTICLE

Here we drive a single particle across the landscape to characterize its motion. The numerical implementation of the landscape is calculated with Eq. 1 as

$$F_y^l(y) = -A_p \sin(2\pi y/\lambda) \tag{5}$$

TABLE I: Simulation parameters and units with comparable experimental values [27].

Quantity	Simulation Unit	Experimental value
length	$a_0 = 1$	$a_0 \sim 1.5\mu m$
energy	$E_0 = 1$	
force	$F_0 = E_0/a_0$	
time	$\tau = \eta a_0/F_0$	
velocity	a_0/τ	$v \sim 5\mu m/s$
driving period	$T = 100\tau$	$T \sim 1.3$ s
viscosity coefficient	$\eta = F_0\tau/a_0$	$\eta \sim 10^{-3}$ Pa-s
substrate period	$\lambda = 1.825a_0$	$\lambda = 3.5\mu m$
substrate amplitude	$U_0 = 0.058E_0$	$U_0 = 25k_BT \sim 2J$
temperature	$T_0 = 0$ [a]	$T \sim 300K$

[a] to learn more about the effects of temperature on this simulation see Ex. IV D where we study the limit $U_0 \sim k_BT$.

where the force is scaled with parameter $A_p = 2\pi U_0/\lambda$. In this section we fix the landscape parameters to $A_p = 0.1F_0$ with $N_p = 20$ minima corresponding to a spatial period $\lambda = 1.825a_0$. The competition between the driving force and landscape potential can produce a variety of hopping patterns in the particle motion. The relative values of F^{ac}, F^{dc} and A_p control the rate and distance a particle moves forward and backward in the landscape. [edit and move:] The addition of an oscillating force can lead to interference effects that create stepped force-velocity curves. Useful model - essentially an overdamped driven pendulum - under certain parameters. The steps occur due to the phase locking between lattice substrate and applied driving force. Step widths depend on AC drive. Discrete modes.

The driven particle moves across the periodic landscape with the same rhythm as the applied time-dependent force $F^D(t)$. When $F^D(t) > A_p$, a particle can overcome the barrier height of the landscape, and the particle hops between minima in the energy landscape. In Fig. 2(a) we plot $F^D(t)$ as a function of time with constants $F^{dc} = 0.1$, $F^{ac} = 0.05$ and $f = 0.01$ cycles per time unit τ. The temporal period of the driving force is $T = 1/f = 100\tau$. We mark the maxima of $F^{ac}(t)$ with the vertical dashed lines – i.e. $\sin(\omega t) = 1$. In Fig. 2(b) we show the $y-$position of the particle as a function of time. We normalize y by λ to show particle motion between substrate minima. The initial particle position is $y = 0$. As the driving force increases, the motion of the particle synchronizes with the driving period T. We measure average particle velocity $\langle v_y \rangle$ as the displacement over the period of the driving force. The particle moves in the positive y-direction through $\Delta y = 2\lambda$ over the time period T, with the average velocity $\langle v_y \rangle = 2\lambda f$. [TODO: update description!] The horizontal dashed lines coincide with the condition the particle is at a substrate minima where substrate force $F^l = -A_p$, i.e. $\sin(\pi y/\lambda) = 1$. The particle synchronizes its motion such that the edriving force is maximum when the landscape force is minimum, as indicated with the intersection of vertical and horizontal lines. The slope of y/λ is proportional to the net force on the particle. This can be seen in Fig. 2 where local extrema appear in y/λ when $F_D(t) \approx 0$.

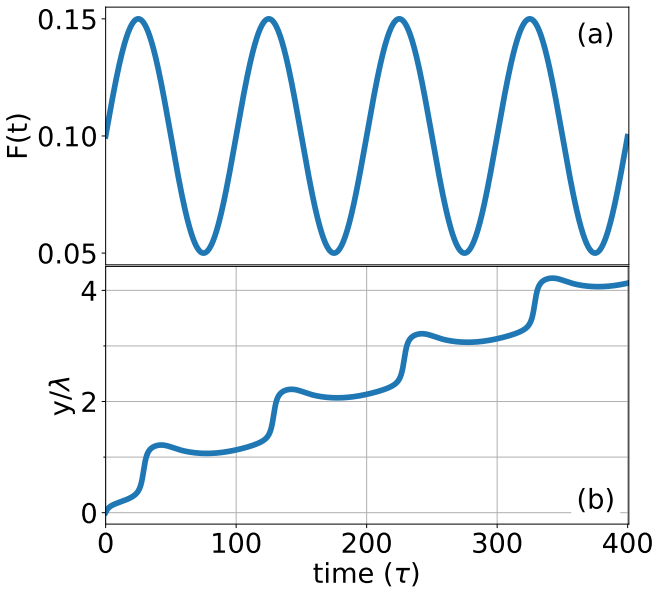

FIG. 2: (a) The applied driving force $F^D(t)$. (b) The $y-$position of the driven particle normalized by the period of the substrate λ.

NOTE: YOUR A_P VALUES ARE TOO SMALL TO MAKE THIS A MEANINGFUL PHASE VARIALBE. YOU NEED TO SCALE WITH THE DRIVE FORCE AMPLITUDES. THIS CAN ALSO HELP YOU UNDERSTAND WHY YOU ARE GETTING BIG JUMPS IN POSITION COMPARED TO JUNIPER ET AL. YOU ARE WORKING IN THE WEAK SUBSTRATE LIMIT. also insert plots of y/λ over a single period with the phase plots - like juniper It is useful to compare mode-locked quantities in a two dimensional phase plot to distinguish fully and partially synchronized behavior. In a non-driven system, an appropriate phase space is particle velocity v_y versus position y. In a system driven parallel to the $y-$direction, we define phase variables to account for the net increase in velocity and position. The phase position is defined as

$$\phi(t) = 2\pi(y(t) - \langle v_y \rangle t)/\lambda \tag{6}$$

centered about the average particle velocity $\langle v_y \rangle$ and normalized by the substrate period λ [27]. In phase diagrams we plot $\phi(t)$ versus the phase velocity

$$\dot{\phi}(t) = 2\pi(v_y(t) - \langle v_y \rangle/\lambda. \tag{7}$$

When velocity is mode-locked to a spatial location a closed loop appears in phase space. The pattern is determined by the mode, or frequency ratio, so a 1:1 mode appears as a circle or oval. Nodes appear in the oval for higher modes, sometimes forming figure-eights or other recognizable patterns. A system that is not fully phase locked will apppear as an unclosed loop. Such quasiperiodic systems are not fully synchronized. With a long simulation time, a quasiperiodic phase diagram fills the plotting region due to the gradual shift in the velocity-position relationship.

In Fig. 3 we plot $\dot{\phi}(t)$ versus $\phi(t)$ for increasing substrate amplitude A_p. We fix the driving force with parameters $F^{dc} = 0.1$ and frequency $f = 0.01$ and $F^{ac} = 0.2$. In Fig. 3(a) there is no substrate ($A_p = 0.0$) and the phase plot is a closed oval centered at $(\phi, \dot{\phi}) = (10, 0)$ with a semimajor axis of $\Delta\phi = 20$ and semiminor axis of $\Delta\dot{\phi} = 2\pi v_{max}/\lambda$. [insert analysis.] As the force from the substrate increases, nodes form in the phase diagram and the motion becomes quasiperiodic so the loops in phase space do not fully overlap. In Fig. 3(b) $A_p = 0.05$ the spatial properties are similar to those in $A_p = 0.0$ with $(\phi, \dot{\phi}) = (10, 0)$ with a semimajor axis of $\Delta\phi = 20$. The dynamical properties are asymmetric, with three nodes in the positive $\dot{\phi}$ values. The thickening of the line indicates the system is not fully synchronized. [insert analysis.] As the substrate force becomes larger, ϕ shifts to lower values and $\dot{\phi}$ to positive values, indicating the particle can only move backward over a short distance. In Fig. 3(c) $A_p = 0.1$ the phase properties are similar to those in $A_p = 0.05$, the three nodes have increased asymmetry in both phase variables $(\phi, \dot{\phi})$. The nodes deepen, indicating [insert analysis.]. In Fig. 3(d) $A_p = 0.2$ the pattern shifts to two nodes, [indicating change analysis]. In Fig. 3(e) $A_p = 0.25$ the system returns to a nodeless orbit, shaped like a triangle [because why?] In Fig. 3(f) $A_p = 0.3$ the particle is trapped between substrate minima, and traces out a small unclosed orbit in phase space [because...] The phase velocity is near zero throughout the motion - [comment on initial conditions]

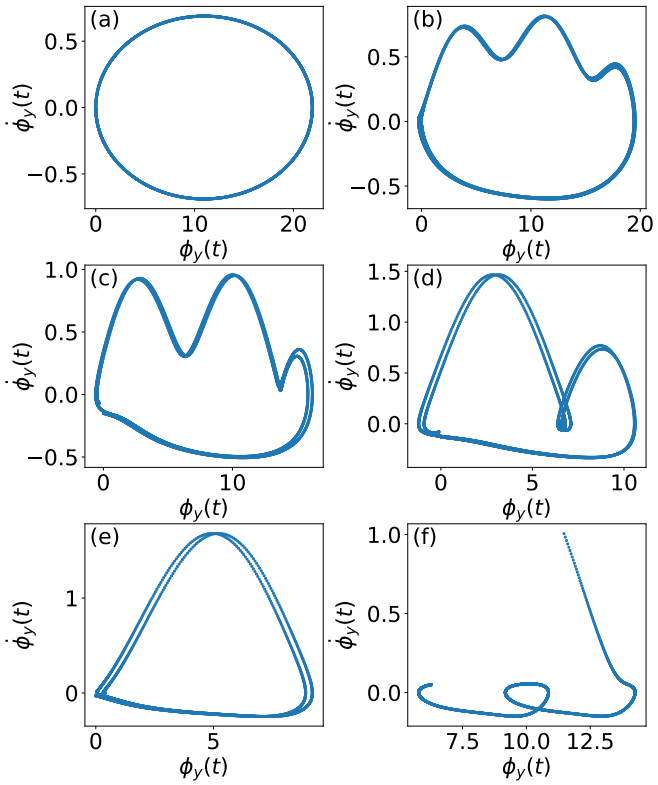

FIG. 3: Phase plot of a particle with the same values of F^{dc} and frequency as Fig. 2. $F^{ac} = 0.2$ and $A_p =$ (a) 0.0, (b) 0.05, (c) 0.1, (d) 0.2, (e) 0.25 and (f) 0.3.

To explore the possible hopping patterns, we sweep through a range of F^{dc} for fixed F^{ac} and A_p to illustrate distinct oscillation modes. A mode is a periodic pattern of hops with a constant average particle velocity, $\langle v_y \rangle$ over a range of driving forces F^{dc}. In Fig. 4 we keep F^{dc} constant for 10^5 simulation timesteps and measure the average velocity $\langle v_y \rangle$ as a function of F^{dc}, with $F^{ac} = 0.05$, $f = 0.01$, and the landscape shown in Fig. 2. The modes appear as discrete steps in $\langle v_y \rangle$ across a range of F^{dc},

Each step represents a different pattern of hops between substrate minima performed by the particle due to the landscape confinement. In Fig. 4 at low F^{dc} the average velocity $\langle v_y \rangle$ is zero. Since A_p is large compared to the extrema of $F^D(t)$, the particle oscillates back and forth in a single minima with no net velocity. At higher F^{dc} the particle velocity $\langle v_y \rangle$ increases in steps of uniform height, $\langle v_y \rangle = n\lambda f$, where n is an integer. The step width is non-linear and can have a variety of interesting patterns such as a devil's staircase related to chaotic dynamics [12]. We note the individual steps are not strictly horizontal since particles move continuously through the landscape, so changes in F^{dc} will create linear changes in net particle displacement that are observable within a single step.

We explore a range of parameters in Ex. IV E where we perform this sweep for several values of F^{ac} including the limiting case that the applied force is a constant value. When $F^{ac} = 0$, no steps appear in the $\langle v_y \rangle$ vs F^{dc} curve. When $F^{dc} - F^{ac} < -A_p$ the particle moves in the negative y-direction during part of the cycle. The period of the substrate can be used to control the net velocity of the dc driven particle, and the applied ac drive can cause mode-locking which appears as non-linear steps in the force-velocity relationship.

In Section IV we explore our model with suggested exercises for interested readers. We include analytic exercises to examine the to linear drag equation in Ex. IV A, the equation of motion in Ex. IV B, and numerical integration techniques in Ex. IV C. We extend the model with numerical exercises to include finite temperature ef-

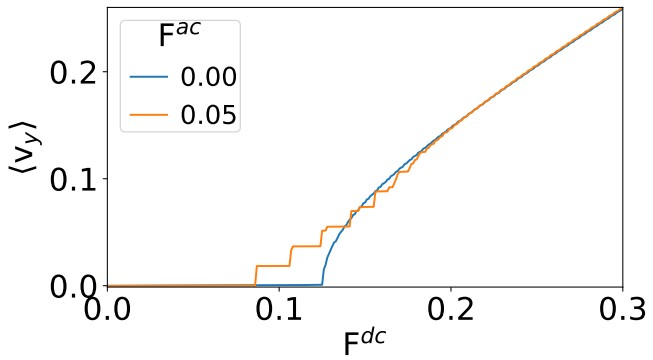

FIG. 4: Average particle velocity $\langle v_y \rangle$ as a function of F^{dc}, the constant parameter of $F^D(t)$ defined in Eq. 2. We fix $F^{ac} = 0.0$ (blue) and $F^{ac} = 0.05$ (orange) with $f = 0.01$ as in Fig. 2.

fects in Ex. IV D. We explore changes in the particle motion with parameter changes in Ex. IV E. Methods to visualize the dynamics of the particle motion are in Ex. IV F.

IV. ASSOCIATED PROBLEMS

A. Drag Models and Reynolds Numbers.

Stokes' law describes the drag force $\vec{F}^{lin} = -3\pi\eta D\vec{v}$ on a sphere moving through a viscous liquid at velocity $\vec{v}$ where η is the dynamic fluid viscosity and D is the particle diameter [38]. In simulation we subsume the constants $3\pi D$ such that $3\pi D\eta \to \eta$. Often drag forces are modeled as a polynomial series [38]

$$\vec{F}^{drag} = -b\vec{v} - cv^2\hat{v} + \dots. \tag{8}$$

Truncating the series to the first term is justified by demonstrating the sphere has a low Reynolds number $R = Dv\rho/\eta$ where ρ is the fluid density and v the particle's speed. When R is small, the quadratic and higher order terms may be ignored in favor of the linear drag term.

Using reasonable values for the experimental analog of this system, show that the Reynolds number is small. In addition to the values listed in Table I, the liquid density ρ varies with temperature with $\rho \sim 10^3$ kg/cm^3 a reasonable first order approximation [41].

B. Equation of Motion

Newton's second law states that the acceleration of a particle i is proportional to the sum of forces on the particle

$$m_i\vec{a}_i = \sum \vec{F}_i \tag{9}$$

where the constant of proportionality is the inertial mass m_i. The addition of a dissipative force to a dynamical equation of colloid motion is typically modeled with a drag force proportional to the particle's velocity in the opposite direction of motion $\vec{F}^{drag} = -\gamma\vec{v}_i$ where $\gamma = 3\pi\eta D$ is the drag coefficient described in Ex. IV A. The ratio of m/γ is known as the momentum relaxation time, and is small for particles with low Reynolds numbers. The mass of the typical experimental colloid particle is 15 picograms, leading to a momentum relaxation time on the order of microseconds. **Confirm for the values listed in Table I, the momentum relaxation time is $m/\gamma \approx 0.5$ μs.**

When m/γ is small, particle acceleration can be ignored entirely. (a) Using Newton's Second Law for a small momentum relaxation time, **show that a particle confined to a landscape exerting force $F^l(\vec{r}_i)$ subject to a time dependent drive $F^D(t)$ can be modeled with the equation of motion described in Eq. 3.**

C. Integration Methods

To calculate the position of the particle we integrate the equation of motion using the standard definition of velocity $\vec{v}_i = d\vec{r}_i/dt$ via the Euler method. Our equation of motion provides a direct calculation for particle velocity, as demonstrated in Ex. IV B. When solving ordinary differential equations, the Euler method is effective for solving linear equations of the form $dy/dt = f(t, y(t))$ with initial condition $y(t_0) = y_0$. The solution is calculated algorithmically by stepping in time through n integer steps $t_n = t_0 + n\Delta t$. At each subsequent step the new value for y is calculated as a map solution using discrete times $y_{n+1} = y_n + f(t_n, y_n)$. **Apply the Euler method to our equation of motion to solve for the analytic expression of position of a particle y_n at the nth timestep (i.e. Eq. 4).**

The Euler method can be applied to non-linear equations effectively if the time step Δt is kept sufficiently small [39]. In our simulations we use the timestep $\Delta t = 0.001$, but we find for a single particle we can just as easily used timesteps $\Delta t = 0.01$ and $\Delta t = 0.1$ over the same maximum time (i.e. decrease the overall simulation time and sampling rate) and reproduce the motions shown in Fig. 2(b). This is due to the linear nature of the solution for an isolated particle. **Demonstrate the simulation timestep can be large with no change to the overall physics in the motion of a single particle.** You will need to modify the maximum simulation time, and the frequency of data saved for plotting purposes.

Interaction with neighboring particles makes a small timestep essential for molecular dynamics simulations. Since particle-particle interactions are typically nonlinear, the interaction force changes significantly over small distances, making this simulation a unique excep-

tion to typical simulation timesteps.

Often molecular dynamics algorithms are solved with higher order methods such as the Verlet or Runge-Kutta methods. These methods include higher order terms that provide accurate solutions for second order differential equations, i.e. $dy/dt = v$ and $dv/dt = f_2(y,t)$. In Newton's second law f_2 would be proportional to the net force on a single particle. In our model we do not integrate $f_2(y,t)$ since $a = dv/dt = 0$, as described in Ex. IV B.

D. Brownian motion

Brownian motion is a phenomena in which visible particles change direction, apparently at random, due to collisions with invisible fluid particles. The rate of collisions depends on the temperature, viscosity amd density of the suspending fluid. At higher temperatures the increased kinetic energy of particles makes collisions more likely, as described by the Maxwell-Boltzmann distribution [42]. An optically trapped colloid executing Brownian motion is a useful probe of microscopic forces [32].

In molecular dynamics simulations it is common to treat the invisible fluid particles as a continuous substance to reduce computational expense. Temperature effects can be modeled by applying randomized forces f^T to the visible particles. We use the normal distristribution from the NumPy random module to generate a series of f_n^T values for each integer timestep n [43]. A normalized random distribution of forces causes fluctuations in motion equally in all directions such that the force f^T averaged over a finite time interval is zero. In one dimension this is expressed as

$$\langle f^T(t)\rangle = \frac{1}{N}\sum_n^N f_n^T = 0 \tag{10}$$

where n is an integer indicating discrete simulation timesteps and $t = N\Delta t$. A particle with sufficient energy k_bT_{min} may hop over landscape barriers. In our simulations, we define temperature as $k_bT/E_0 \to T$ with constants set to unity to compare directly with force.

With no applied driving force, find the minimum temperature required for a single particle to hop over maxima in the potential landscape. Assume the particle is confined to move along the $y-$direction, include Brownian motion in the model. In Fig. 5, we demonstrate the transition from pinned to hopping in a non-driven colloid for $T/A_p = 3.0$, 3.5, and 4.0.

In Fig. 5 we show the position versus time of a particle confined to a sinusoidal landscape undergoing Brownian motion. We increase the temperature relative to the amplitude of the landscape troughs until the particle enters a hopping regime. In Fig. 5(a) the temperature is $T/A_p = 4.0$. The particle executes a random walk centered at the potential minima $y/\lambda = 10$. We ran many simulations and never observed a hop to another minima within this simulation time. In Fig. 5(b) $T/A_p = 5.0$, hops between potential minima are possible but not probable, a back-forth hop occurs from $y/\lambda = 10$ to 12 at $t \sim 40000\tau$ and a single hop from $y/\lambda = 10$ to 8 occurs at $t \sim 280000\tau$. In other simulations with identical parameters, we sometimes observed no hops or two hops between minima, as expected with random fluctuating systems. In Fig. 5(c) $T/A_p = 6.0$ we observe many hops. The random thermalized kicks are sufficiently large to make the particle perform what appears to be a random walk of hops atop the substrate. [prove it]

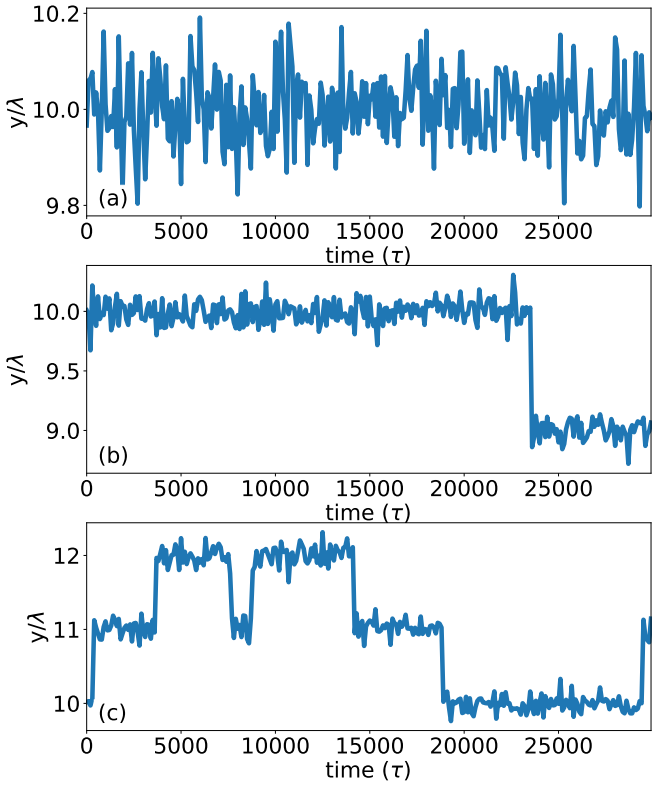

FIG. 5: Motion of a particle undergoing Brownian motion on a washboard potential energy landscape. (a) $T/A_p = 3.0$ no hopping occurs. (b) $T/A_p = 3.5$ one hop occurs and (c) $T/A_p = 4.0$ many hops occur. Note the scale of the $y-$axis differs in each panel and the time scale is greater than in Fig. 2. The precise timing of hops pattern varies by simulation, sometimes exhibiting several hops for $T/A_p = 3.5$.

For a driven particle, we ignore the effects of temperature in these simulations. We note that even at $T/A_p = 6.0$ the hopping rate is much less than the frequency of the applied drive. This can be seen in the time scale in Fig. 5, where the average hopping rate is approximately every 15000τ, a value much larger than $T = 100\tau$. At sufficiently high temperatures, Brownian motion does affect the formation of mode-locked steps and can be observed in experiments. [explore]

E. Exploring Parameters of the Model

A range of oscillation behaviors can be explored by varying the relative strength of the confining landscape and external driving force. For the single driven particle, the hopping patterns are typically characterized by n_f the number of steps forward versus n_b the number of steps backward within a single time period. The total displacement of $(n_f - n_b)\lambda$ is the net hop length. In Fig. 2, the particle moves forward through two minima ($n_f = 2$), and does not move backward a full minima ($n_b = 0$). In order to achieve backwards hops, the driving parameters must have a ratio of $F^{ac}/F^{dc} > 1$ and a difference $|F^{ac} - F^{dc}| > A_p$. The frequency must be sufficiently low so that the applied force is large over a sustained time interval, allowing a particle to hop a substrate maxima. **Explore the effect changing the driving frequency on the hopping pattern.**

Fig. 6 shows the effects of lowering the frequency of applied driving force We hold the remaining parameters fixed to $F^{dc} = 0.1$, $F^{ac} = 0.05$, and $A_p = 0.1$. We observe no backward steps ($n_b = 0$) across a broad range of frequencies since $F^{dc} - F^{ac} = 0.05$ is too small to overcome A_p. The rate of forward hops increases as frequency decreases, but in each case the particle hops across two substrate periods as in Fig. 2. In Fig. 6(a-b) the particle hopping rate do not match the temporal period of $F^D(t)$ due to the high frequency. In Fig. 6(a) the high frequency $f = 0.1$ is apparent in the undulations of the particle with a period of 10τ. The particle is trapped between substrate minima $y \approx \lambda/2$ for a time interval of 400τ. In Fig. 6(b) the frequency $f = 0.05$ with a period of 20τ arrests the particle between minima, with a hopping rate of 200τ. At intermediate frequencies such as $f = 0.01$ the particles are synchronized so that the hopping rate matches the driving frequency. In Fig. 6(c) $f = 0.015$ the particle hops forward two minima every 67τ. Low frequencies result in sustained positive motion of a particle. In Fig. 6(d) $f = 0.005$ the particle executes two subsequent forward hops before becoming trapped for the remainder of the period 200τ. In Fig. 6(e) $f = 0.001$ the hopping is continuous over the simulation time. Here the particle reaches the top edge of the system and wraps back to $y = 0$. Given a simulation time of the period length 1000τ, the particle would cease forward motion.

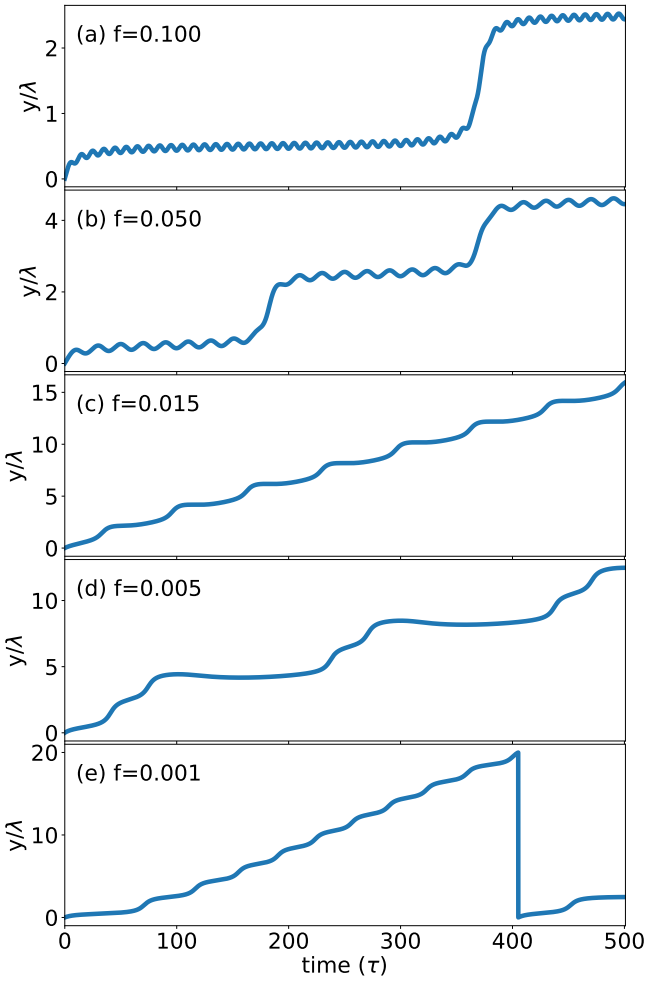

FIG. 6: Motion of a particle with the same values of $F^{dc} = 0.1$ and $F^{ac} = 0.05$ as Fig. 2 and decreasing frequency $f =$ (a) 0.1, (b) 0.05, (c) 0.015, (d) 0.005 and (e) 0.001 where the particle wraps the periodic boundary conditions.

Hopping patterns with backward steps are more difficult to achieve than forward. In Ref.[27] experiments with single colloids produce the following combinations of forward and backwards steps: $n_f = 0$ to 6 for $n_b = 0$, $n_f = 0$ to 5 for $n_b = -1$, and $n_f = 2$ to 3 for $n_b = -2$ by sweeping through a variety of applied forces parameters F^{dc} and F^{ac}. **Find the parameters that create hopping patterns similar to those in Ref. [27].**

In Fig. 7 we explore a hopping pattern not observed in Ref. [27]. This is possible in simulation because our particle readily hops through 2λ. We fix $f = 0.01$, $F^{dc} = 0.1$, and $A_p = 0.1$ and increase the amplitude of F^{ac}, which causes the number of backwards steps to increase. The number of forward steps also increases due to the increased total positive amplitude of $F^D(t)$. In Fig. 7(a) $F^{ac} = 0.2$. the number of backwards steps $n_b = 0$ with $n_f = 6$. In Fig. 7(b) $n_b = 2$ and $n_f = 8$. In Fig. 7(c) $n_b = 4$ and $n_f = 10$. In each case the average velocity is $\langle v_y \rangle = 6\lambda/T$.

In Fig. 8 we sweep the constant driving force F^{dc} for a fixed amplitude F^{ac} and frequency. Fig. 8(a) shows $F^{ac} = 0.0$ and (b) shows $F^{ac} = 0.4$ with frequency $f = 0.01$. With no oscillating component of the driving force, the force-velocity relationship is monotonically increasing above the depinning threshold F^c such that

$$\langle v_y \rangle \propto (F^{dc} - F^c)^{-\beta}. \tag{11}$$

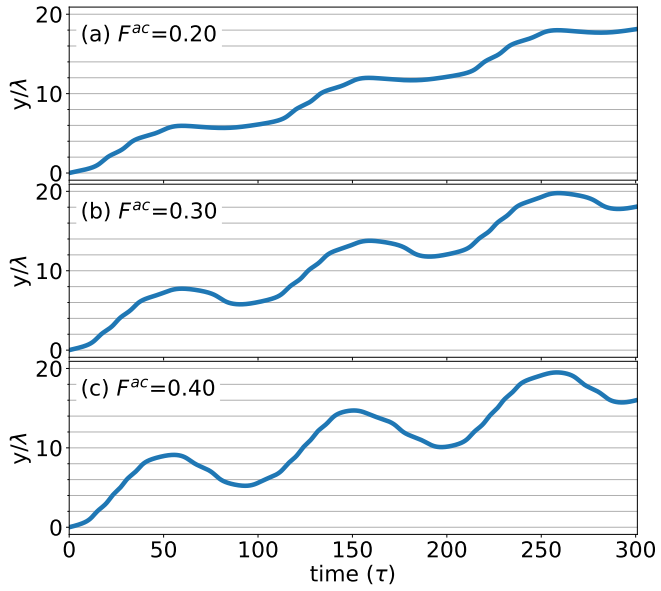

FIG. 7: Motion of a particle with the same values of F^{dc} and frequency as Fig. 2 and increasing F^{ac}. (a) The particle moves forward six minima with no steps backward. (b) The particle moves forward eight minima with two steps backward. (c) The particle moves forward nine minima with four steps backward.

The critical force F^c is equal to the maximum substrate force A_p so the applied driving force can move a particle over a substrate barrier. The particle does not phase lock since there is no periodicity to $F^D(t)$, but does exhibit undulations in $\langle v_y \rangle$ due to the corregations in the substrate. When $F^{ac} = 0.4$, mode-locked steps appear in $\langle v_y \rangle$ vs. F^{dc}. At low values of F^{dc} the particle may move backwards, distorting the steps, as seen below $F^{dc} < 0.3$ Between $0.3 < F^{dc} < 0.5$ the system exhibits phase locked steps.

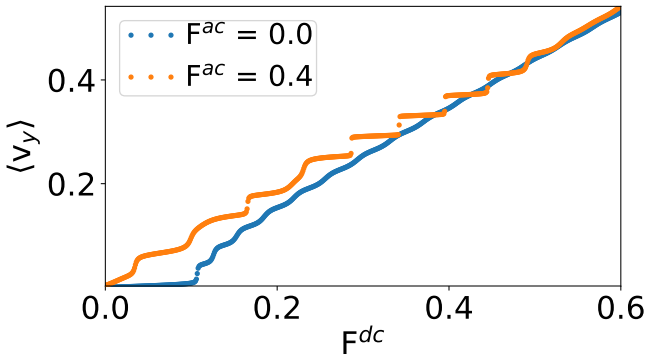

FIG. 8: $\langle v_y \rangle$ vs. F^{dc} of a particle with $F^{ac} = 0.0$ (blue) and $F^{ac} = 0.4$ (orange) with frequency $f = 0.01$. The substrate is as in Fig. 2 with $A_p = 0.1$.

F. Visualizing motion

Drawing the contour

The code for generating a two dimensional colored plot of the potential landscape is calculated by evaluating the analytic function in Eq. 1 for a grid of values (x_n, y_n).

I have python code that does all of this, but I don't have it set up to play nice with my new python MD code

Also the animation library in python...

V. CONCLUSION

A single particle driven across a periodic potential landscape synchronizes its motion to environmental and external forces, a phenomena known as mode-locking. Our simulations reproduce experiments presented in Juniper *et al.* [27] of mode locking in driven colloids on a periodic optical landscape. Colloids are relatively easy to manipulate and image in experiments, making ideal proxies for systems such as cold atoms or electron gases [30]. Dynamical mode-locking is observed important technologies such as in quantum electronic devices as stepped regions in current-voltage (I-V) relationship, where voltage is the analog of external driving force and current is that of particle velocity. Known as Shapiro steps, these mode-locked or phase-locked currents have been observed due to applied ac voltages in single Josephson junctions [20, 23] and coupled arrays of junctions [21]. Shapiro steps vary in width depending on the strength of the applied ac forces, and are observed in a variety of ac and dc driven systems displaying non-Ohmic behavior in voltage-current curves, including charge waves, spin density waves and superconducting vortices in landscapes engineered with periodic patterns of pinning sites [22]. Mode-locking is a useful probe of complex quantum mechanical systems since the motions of individual particles can only be inferred from other measurements. Our results can be relevant to synchronization effects in a broad range of experiments systems including optically confined colloids, superconductors with periodic pinning arrays, and the charge and spin of atomic systems.

Acknowledgments

We acknowledge Harvey Gould and Jan Tobochnik, who invited us to write the article and supported its development. Charles and Cynthia Reichhardt advised the project and provided the original molecular dynamics code written in the C programming language. We acknowledge funding from the M.J. Murdock Charitable Trust and the Pacific Research Institute for Science and Mathematics.

[1] A. Pikovsky, M. Rosenblum, and J. Kurths, *Synchronization: A Universal Concept in Nonlinear Sciences* (Cambridge Univ. Press, Cambridge, 2003).

[2] M. Bennett, M.F. Schatz, H. Rockwood, and K. Wiesenfeld, Huygens' clocks, Proc. Roy. Soc. A **458**, 563 (2002).

[3] K. Okamoto, A. Kijima, Y. Umeno, and H. Shima. Synchronization in flickering of three-coupled candle flames. Sci Rep **6**, 36145 (2016)

[4] T. Arane, A. K. R. Musalem and M. Fridman, Coupling between two singing wineglasses, Am. J. Phys. **77**, 1066 (2009).

[5] J. Jia, Z. Song, W. Liu, J. Kurths, and Xiao, J. Experimental study of the triplet synchronization of coupled nonidentical mechanical metronomes. Sci. Rep. **5**, 17008 (2015).

[6] S. Portugal, T. Hubel, J. Fritz, S. Heese, D. Trobe, B. Voelkl, S. Hailes, A. M. Wilson and J. R. Usherwood. Upwash exploitation and downwash avoidance by flap phasing in ibis formation flight. Nature **505**, 399 (2014).

[7] I. Aihara, T. Mizumoto, T. Otsuka, H. Awano, K. Nagira, H. G. Okuno and K. Aihara. Spatio-Temporal Dynamics in Collective Frog Choruses Examined by Mathematical Modeling and Field Observations. Sci Rep **4**, 3891 (2014).

[8] P. Tranchant, D. T. Vuvan, and I. Peretz, Keeping the Beat: A Large Sample Study of Bouncing and Clapping to Music. PLoS ONE 11(7): e0160178. (2016).

[9] G. Martin Hall, Sonya Bahar, and Daniel J. Gauthier, Prevalence of Rate-Dependent Behaviors in Cardiac Muscle. Phys. Rev. Lett. **82**, 2995 (1999).

[10] W. Singer. Striving for coherence. Nature, **397** 391, 1999.

[11] Dutta, S., Parihar, A., Khanna, A. et al. Programmable coupled oscillators for synchronized locomotion. Nat Commun **10**, 3299 (2019).

[12] P. Bak. The Devil's Staircase. Physics Today **39**, 12, 38 (1986).

[13] J. A. Lissajous. "Mmoire sur l'Etude optique des mouvements vibratoires," Annales de chimie et de physique, 3rd series, 51 (1857) 147-232

[14] E. Y. C. Tong, Lissajous figures, The Physics Teacher **35**, 491 (1997).

[15] A. Pertsinidis, and X. Ling, Equilibrium Configurations and Energetics of Point Defects in Two-Dimensional Colloidal Crystals. *Phys Rev Lett*, **87**, 098303 (2001).

[16] E. M. Purcell, Life at low Reynolds numbers, Am. J. Phys. **45**, 311 (1977).

[17] B. D. Josephson, Phys. Letters **16**, 25 (1962).

[18] B. D. Josephson, Advan. Phys. **14**, 419 (1965).

[19] W. C. Stewart, Current-Voltage Characteristics of Josephson Junctions, Appl. Phys. Lett. 12, 277 (1968).

[20] S. Shapiro, Josephson currents in superconducting tunneling: the effect of microwaves and other observations, Phys. Rev. Lett. 11, 80 (1963).

[21] S. P. Benz, M. S. Rzchowski, M. Tinkham, and C. J. Lobb, Fractional giant Shapiro steps and spatially correlated phase motion in 2D Josephson arrays, Phys. Rev. Lett. 64, 693 (1990); D. Domnguez and J. V. Jose, Giant Shapiro steps with screening currents, Phys. Rev. Lett. 69, 514 (1992).

[22] C. Reichhardt, R. T. Scalettar, G. T., Zimányi, N. Grønbech-Jensen, Phase-locking of vortex lattices interacting with periodic pinning. Phys. Rev. B **61**, R11914 (2000).

[23] A. A. Golubov, M. Yu. Kupriyanov, and E. Ilìchev. The current-phase relation in Josephson junctions, Rev. Mod. Phys. **76**, 411 (2004).

[24] Dengling Zhang, Haibo Qiu, and Antonio Muñoz Mateo, Unlocked-relative-phase states in arrays of Bose-Einstein condensates, Phys. Rev. A **101**, 063623 (2020).

[25] C. Reichhardt and C. J. Olson Reichhardt, Depinning and nonequilibrium dynamic phases of particle assemblies driven over random and ordered substrates: a review, Rep. Prog. Phys. 80, 026501 (2017).

[26] C. Reichhardt, and C. J. O. Reichhardt, Shapiro steps for skyrmion motion on a washboard potential with longitudinal and transverse ac drives. Phys. Rev. B **92**, (22). (2015).

[27] M. P. N. Juniper, A. V. Straube, R. Besseling, D. G. A. L. Aarts, and R. P. A. Dullens, Microscopic dynamics of synchronization in driven colloids. Nat. Commun. 6, 7187 (2015); Juniper, M. P. N., Zimmermann, U., Straube, A. V., Besseling, R., Aarts, D. G. A. L., Lwen, H., and Dullens, R. P. A. Dynamic mode locking in a driven colloidal system: Experiments and theory. New Journal of Physics, 19(1). (2017).

[28] S. Herrera-Velarde and R. Castaeda-Priego, Superparamagnetic colloids confined in narrow corrugated substrates, Phys. Rev. E **77**, 041407 (2008).

[29] S. Herrera-Velarde and R. Castaeda-Priego, J. Phys.: Condens. Matter 19, 226215 (2007).

[30] D. G. Grier, A revolution in optical manipulation. Nature **424**, 810 (2003).

[31] Arthur Ashkin, Optical trapping and manipulation of neutral particles using lasers, Proc. Natl. Acad. Sci. U.S.A. 94, 48534860 (1997).

[32] G. Volpe and G. Volpe, Simulation of a Brownian particle in an optical trap, Am. J. Phys. 81 (3), March 2013

[33] C. Lutz, M. Kollmann, and C. Bechinger, Phys. Rev. Lett. **93**, 026001 (2004); C. Lutz, M. Kollmann, C. Bechinger, and P. Leiderer, J. Phys.: Condens. Matter **16**, S4075 (2004).

[34] S. Tarucha, T. Honda, T. Saku, Solid State Commun. 1995, 94, 413.

[35] A. Gholami, O. Steinbock, V. Zykov, and E. Bodenschatz, Flow-Driven Waves and Phase-Locked Self-Organization in Quasi-One-Dimensional Colonies of Dictyostelium discoideum, Phys. Rev. Lett. **114**, 018103 (2015).

[36] D. Frenkel and B. Smit, Understanding Molecular Simulation: From Algorithms to Applications (Academic Press, London, 2001).

[37] M. P. Allen and D. J. Tildesley, Computer Simulation of Liquids. Second Edition. Oxford University Press (2017).

[38] J. Taylor, Classical mechanics. University Science Books (2005).

[39] M. Newman, Computational Physics, CreateSpace Independent Publishing Platform. (2012).

[40] Supplementary videos coming soon.

[41] IAPWS R12-08, Release on the IAPWS Formulation 2008 for the Viscosity of Ordinary Water Substance, September 2008, http://www.iapws.org/relguide/viscosity.html

[42] A Einstein, Investigations on the Theory of the Brownian

Movement, Dover Publications (1956).
[43] Harris, C.R., Millman, K.J., van der Walt, S.J. et al. Array programming with NumPy. Nature **585**, 357 (2020).